Title
Influence of anisotropic stress states on the thermal volume change of unsaturated silt

Journal
Soils and Foundations, 57(2)

ISSN
0385-1621

Authors
Shanina, Mahmud
McCartney, John S

Publication Date
2017-04-01

DOI
10.1016/j.sandf.2016.12.003

Peer reviewed

Manuscript

IMPACT OF ANISOTROPIC STRESS STATES ON THE THERMAL VOLUME CHANGE OF UNSATURATED SILT

by Mahmud Shanina, Ph.D.[1] and John S. McCartney, Ph.D., P.E.[2]

Abstract: This study is focused on understanding the influence of anisotropic stress states on the thermal volume change of unsaturated, compacted silt specimens. A thermo-hydro-mechanical true-triaxial cell was used that permits control of the temperature on all six boundaries of a cubical soil specimen as well as control of the suction within the specimen to provide drained conditions during mechanical loading and temperature changes. Six non-isothermal tests were performed as part of this study, each involving suction application, consolidation to a given isotropic or anisotropic stress state, heating and cooling in stages under drained conditions, and unloading. Specifically, tests having minor to major principal stress ratios of 1.0, 0.7, and 0.5 were performed on specimens having initial degrees of saturation of 0.7 and 0.8, complementing tests on the same soil under similar stress states but saturated conditions published in a previous study. Although compressive thermal axial strains were measured in both the major and minor stress directions, a greater thermal axial strain was observed in the direction of the major principal stress for stress ratios less than 1.0. However, similar thermal volumetric strains were observed in all of the tests regardless of the stress state. A small effect of inherent anisotropy was observed due to the formation of the specimen using compaction. Specimens with a lower initial degrees of saturation experienced greater thermal volume changes than specimens closer to saturation, possibly due to thermal collapse of the air-filled voids during heating or thermally accelerated creep after application of a given plastic strain during mechanical loading. An empirical relationship to consider the effects of anisotropic stress states

[1] Professor, University of Misurata, Dept. of Civil Engineering, Libya; Mahmud.shanina@colorado.edu
[2] Associate Professor, University of California San Diego, Department of Structural Engineering. 9500 Gilman Dr., La Jolla, CA 92093-0085, mccartney@ucsd.edu.

and variable saturation was incorporated into an established elasto-plastic model developed for saturated soils under isotropic conditions, and a good fit was obtained between the measurements and predictions.

INTRODUCTION

A technique used to improve the energy efficiency of heat pumps for building heating and cooling systems is to embed closed-loop heat exchangers into drilled shaft foundations to form energy piles (Brandl 2006; Laloui et al. 2006; Adam and Markiewicz 2009; McCartney 2011; Murphy and McCartney 2015; Murphy et al. 2015). Heat can be transferred to and from the ground by circulating fluid through the heat exchangers. When the soil surrounding the energy pile changes in temperature, potentially irreversible soil volume changes may occur depending on the stress state, soil mineralogy, and degree of saturation (Campanella and Mitchell 1968; Demars and Charles 1982; Hueckel and Baldi 1990; Towhata et al. 1993; Burghignoli et al. 2000; Delage et al. 2000; Sultan et al. 2002; Romero et al. 2003; Cekerevac and Laloui 2004; Salager et al. 2007; Uchaipichat and Khalili 2009; McCartney 2012; Vega and McCartney 2015; Alsherif and McCartney 2015; Coccia and McCartney 2012, 2016a, 2016b). These thermal volume changes may affect the lateral stress distribution along the energy foundation, and may lead to relative movement between the energy pile and surrounding soil (Vega and McCartney 2015). Although constitutive models are available to consider the thermal volume change of soils (Hueckel and Pellegrino 1989; Hueckel and Borsetto 1990; Cui et al. 2000; Laloui and Cekeravac 2003; Abuel-Naga et al. 2009), an isotropic stress state is assumed. Accordingly, the same thermal expansion or contraction is assumed to occur in both the major principal stress (vertical) and minor principal stress (horizontal) directions when simulating the behavior of soils surrounding energy piles. Despite the experimental data available on the recoverable and permanent deformations of unsaturated soil during heating and cooling, the influence of anisotropic stress states on the thermal deformation of unsaturated soils still needs to be better understood before constitutive relationships thermal volume change of soils can be incorporated into design methods for energy piles such as that of Knellwolf et al. (2011).

Coccia and McCartney (2012) studied the effect of anisotropic stress states on the thermal volume change of saturated specimens of compacted Bonny silt using a specially-designed thermo-hydro-mechanical (THM) true-triaxial cell. The results from their testing program showed that the anisotropic stress state does not have a significant influence on the thermally-induced volumetric strain. However, the initial anisotropic stress state does have a significant influence on the magnitude and trend of thermal axial strains in the directions of the major and minor principal stresses. Specifically, during drained heating of anisotropically-consolidated cubical specimens isotropically compressed to normally consolidated conditions before being unloaded in the minor principal stress direction, plastic contraction was observed in the major principal stress direction while less contraction (or even expansion) was observed in the minor principal stress direction. The difference in the thermal axial strains was found to depend on the ratio of the minor to major principal stresses (referred to as the stress ratio K). Coccia and McCartney (2012) proposed that the plastic contraction in the major principal stress direction was because the stress was still at the maximum stress level encountered in that direction, while the lower plastic contraction or expansion in the minor principal stress direction was due to the stress history in that direction that made the behavior similar to an overconsolidated soil.

In addition to the need to perform more in-depth testing to fully understand the influence of anisotropic stress states on the thermal volume change of soils, there are opportunities to improve the experimental approach involving the THM true-triaxial cell used by Coccia and

McCartney (2012). They had intended to perform their tests in plane strain conditions, but found that the thermal expansion of the cell during heating may have led to changes in the intermediate principal stress and strain values. They also only heated the specimen on two opposing faces, requiring a long heating period to reach thermal equilibrium. Accordingly, efforts were made in this study to implement better control of the principal stresses and temperatures applied to each face during testing. Another issue with the approach used by Coccia and McCartney (2012) is that the unloading of the specimen in the minor principal stress direction may have led to a decrease in the mean stress, which may have led to a slight overconsolidation effect in the specimen which could have potentially affected the trends in the thermal volumetric strain. A better approach would be to increase the major principal stress to reach an anisotropic stress state so that the mean stress increases but still remains in normally consolidated conditions. Finally, although Coccia and McCartney (2012) designed their true-triaxial cell with the capability to evaluate unsaturated conditions, they only focused on the behavior of saturated specimens meaning that their work could be complimented by investigations using this feature.

BACKGROUND

Previous studies have observed that the overconsolidation ratio (OCR) has a significant effect on the thermal volume change of a soil specimen when heated under a constant mean stress in drained conditions. Soils with larger OCR values trend to expand during heating while soils with lower OCR values trend to contract (Baldi et al. 1988; Towhata et al. 1993; Cekerevac and Laloui 2004; Sultan et al. 2002; Abuel-Naga et al. 2007; Vega and McCartney 2015). For example, Cekeravac and Laloui (2004) observed thermal contraction for saturated kaolinite clay specimens with OCR values between 1 and 2 while thermal expansion was observed for specimens at higher values of OCR of values 6 and 12 (although these specimens were observed to contract after reaching a certain temperature). Although there have not been many studies on the thermal volume change of soils under anisotropic stress states except that of Coccia and McCartney (2012), Hueckel and Pellegrini (1996) found that inherent anisotropy arising from the orientation of clay particles perpendicular to the direction of consolidation or compaction may lead to greater lateral thermal axial strains than vertical thermal axial strains in saturated clays for heating under isotropic stress states.

The effect of temperature on the volume change behavior of unsaturated soils has been evaluated in several studies (Romero et al. 2003; Francois et al. 2007; Salager et al. 2008; Tang et al. 2008; Uchaipichat and Khalili 2009; McCartney 2012; Alsherif and McCartney 2015). Uchipichat and Khalili (2009) studied the effect of the thermal volume change of normally consolidated and overconsolidated soils having constant suction conditions. Similar to saturated soils, they observed thermal expansion in overconsolidated specimens during drained heating-cooling tests between 25 to 60 °C, but observed contraction under lower overconsolidation ratios. They did not observe a significant effect of the initial degree of saturation on the thermal volume change, but the fact that several different stress paths were applied to the specimens before heating may have affected the influence of this variable. Alsherif and McCartney (2015) performed heating tests on compacted Bonny silt at low suction (0.04 MPa) and high suction (300 MPa) magnitudes, and found that soils heated under low suction contract but those at high suctions expand. Their results were reinterpreted by Alsherif and McCartney (2016) in terms of the mean effective stress and OCR, and it was observed that the trends are similar to those for saturated specimens of compacted Bonny silt tested by Vega and McCartney (2015).

MATERIAL

Bonny silt was used in this study as its thermal volume change has been investigated under different stress states and degrees of saturation in previous studies (Coccia and McCartney 2012; Vega and McCartney 2015; Alsherif and McCartney 2015). Bonny silt has a fines fraction of 83%, a liquid limit of 25, and plastic limit of 21, so it is classified as ML (inorganic low plasticity silt) according to the Unified Soil Classification Scheme (USCS). The specific gravity of the particles is 2.65. The specimens tested in this study were prepared using compaction in order to reach initial degrees of saturation of 0.7 and 0.8. All cubical soil specimens were prepared using static compaction to reach the same initial dry unit weight of 16.2 kN/m^3, which corresponds to an initial void ratio of 0.59. This dry unit weight corresponds with about 98% of the maximum dry unit weight from the standard Proctor compaction curve (16.6 kN/m^3). The target gravimetric water content values investigated in this study were 15.5 and 17.5%, which correspond to initial degrees of saturation of 70% and 80%, respectively, and are both wet of the optimal gravimetric water content for the standard Proctor compaction effort (14%).

Before compaction, the soil was mixed with water until the target gravimetric water content was reached. It was then sealed within a five-gallon bucket for 24 hours to allow the water content to homogenize within the soil. A mechanical press was used to compress the specimen in six lifts of equal height within a cubical aluminum mold having a side length of 178 mm. The under-compaction technique was used to ensure uniform compaction of the specimen. The top of each compacted lift was scarified to minimize any potentially weak planes within the cubical specimen. To remove the specimen from the mold, the specimen was first pushed from the mold using the press before removing the side walls so that this process does not pull on the surfaces of the specimen. The compacted specimen was covered immediately with plastic wrap to avoid changes in the degree of saturation while the rest of the components of the cubical cell were being assembled. Pictures of the mold and specimen during and after preparation are presented by Shanina (2015).

EXPERIMENTAL APPROACH

Experimental Setup

The true-triaxial cell used in this study was originally developed by Mould (1983) and updated by Takata (2000). In its typical configuration, this cell uses six flexible latex bladders reacting against aluminum mechanical loading plates to apply principal stresses to the faces of a cubical soil specimen, following the approach outlined by Ko and Scott (1967). The deformations of each face of the true-triaxial cell are measured using spring-loaded linearly variable differential transformers (LVDTs). Coccia and McCartney (2012) adapted the cell for thermo-hydro-mechanical testing by replacing the bottom and top faces of the cell with rigid face plates. This study used replaced only the bottom face of the cell with a rigid face plate, similar to the approach of Hoyos and Macari (2001), Hoyos et al. (2008), and Hoyos et al. (2012). As shown in the cross-section schematics of the true-triaxial cell in Figures 1(a) and 1(b), the bottom face in the z-direction is a rigid face plate that contains porous disks that independently apply pore air pressure (u_a) or water pressures (u_w), while the other faces in the x-and y-directions are flexible bladders that are used to apply total principal stresses. The bottom rigid face plate incorporates heating elements to control temperature on this face of the specimen and hydraulic ports to control the pore water and air pressures within the specimen (or to provide drainage during mechanical loading or changes in temperature). This rigid face plate is referred to as a hydro-thermal face plate.

This study involved additional modifications to the THM true-triaxial cell to address some of the issues encountered by Coccia and McCartney (2012). First, the THM true-triaxial cell was configured to apply principal stresses in all three orthogonal directions by maintaining a mechanical loading plate on the z_1 face of the cell, as shown in Figure 1(a). This permits application of anisotropic stress states to a cubical soil specimen that correspond with the bedding planes associated with compaction of the soil specimen (i.e., major principal stress in the vertical direction orthogonal to the bedding planes and minor principal stresses applied equally in the two horizontal directions parallel to the bedding planes). This approach also permits independent measurement of the principal strains in all three orthogonal directions. Further, the modified system permits incorporation of temperature control on each face of the cell by circulating pressurized, heated water through five of the bladders and circulating water through the heating elements in the hydro-thermal face plates. This uniform heating permitted thermal equilibrium to be reached in a shorter period of time than the approach of Coccia and McCartney (2012).

Although the particular anisotropic stress state investigated in this study (stress in the vertical direction equal to the major principal stress, and stresses in the two horizontal directions equal to each other and corresponding to the minor and intermediate principal stresses) correspond to a triaxial compression stress state that could be investigated in an advanced thermal triaxial cell, there are several advantages for using this advanced testing device. First, the cubical cell permits tests to be performed in stress-control conditions. This is desired when measuring thermal volume changes so that the device does not provide displacement constraints on the specimen that could lead to a change in stress state in the specimen. This can only be achieved in a triaxial frame with feedback control or incorporating a pneumatic piston to control the axial stress such as that used by Alsherif and McCartney (2015). The cell also permits evaluation of much larger specimens than in a conventional triaxial cell which better permits better assessment of inherent anisotropy effects in compacted specimens due to the larger sample size. Even though the thermal axial strains may be similar in experiments performed in the true-triaxial cell and in a conventional triaxial cell, a larger specimen will have larger deformations that are easier to measure within the sensitivity of available measurement systems.

The pore water pressures are applied through a high air-entry (HAE) porous ceramic disk that only allows water to pass until reaching a suction of 300 kPa. The pore air pressures are applied through coarse porous disks that have a very low air entry suction (less than 0.1 kPa). Matric suction in the specimens can either be measured or controlled using the ports at the base of the cell. To measure the matric suction, the air pressure is maintained at atmospheric conditions and the pressure in the water reservoir behind the HAE ceramic disk is measured in the same manner as a tensiometer. Specifically, the water pressure within the reservoir beneath the HAE ceramic disk was monitored using a pressure sensor. If a compacted soil is placed atop the ceramic disk, there will be a tendency to draw water through the disk into the specimen due to the gradient formed by the initial suction in the specimen. Negative water pressures up to approximately -80 kPa can be measured using this approach. At equilibrium, the negative water pressure measured within the reservoir is expected to be approximately equal to the suction within the unsaturated specimen as the pore air pressure is assumed to be zero.

Alternatively, the suction can be controlled using the axis translation technique (Hilf 1956). In this case, positive pore air and water pressures can be applied independently to the base of the specimen through the low air entry and high air entry disks, respectively, with a difference (u_a – u_w) being equal to the matric suction in the specimen. Although it is straightforward to control the suction in the specimen to provide drained conditions, the particular configuration evaluated in this study shown in Figure 1(a) is not optimal for changing the suction in the specimen because water must flow from the bottom face of the specimen to the upper corners of the specimen through capillarity, which can be time consuming and may lead to air entrapment. Accordingly, the approach used in this study is to measure the initial suction in the compacted specimen using the tensiometer approach, and then subsequently apply this same suction using the axis translation technique to permit drained mechanical compression and drained heating experiments to be performed. This approach avoids the need to wait for complicated water flow processes before applying thermo-mechanical loads to the specimen. Although this approach may be affected by the different soil structures induced by compaction, both initial degrees of saturation investigated in this study correspond to compaction wet of optimum so the soil structure soil not be a major factor.

It should be noted that during transient heating of the specimen, the results from this test cannot be considered to be representative of an element test because the temperature distribution may not be uniform through the volume of the cubical specimen. To investigate the transient heating response, the cubical specimen should be treated as a boundary value problem, as noted by Zhang and Kurimoto (2016). However, at equilibrium it is assumed that the temperature, suction, and degree of saturation will be uniform throughout the cubical specimen and that the results will be representative of an element test. Accordingly, the heating approach used in this study is to apply changes in temperature in stages to obtain equilibrium volume changes that correspond to a uniform change in temperature across the volume of the cubical specimen.

Machine Deflection Evaluation

Before performing tests on the soil, it is necessary to characterize the deflections of the THM true-triaxial cell during changes in stress or temperature. Although the true-triaxial cell was designed to be as rigid as possible, application of stresses to the specimen will cause the space frame to expand outward which may affect the displacement measurements of the LVDTs. The approach used to evaluate the mechanical and thermal machine deflections was to first perform tests on an aluminum cube having known mechanical and thermal properties. The mechanical machine deflections were calculated by subtracting the elastic deflection of the aluminum cube from the average deflections of the LVDTs mounted on the face plates. The deflection of the aluminum cube was calculated as follows:

$$\delta = \frac{\sigma \times L}{E} \qquad (1)$$

where δ is the elastic deflection of the aluminum cube, σ is the axial stress in kPa, L is the length of the aluminum cube, which is equal to 178 mm and E is the Young's modulus of the aluminum cube, which is equal to 69 GPa. A positive machine deflection is defined as compression. The slopes of the machine deflections in each principal stress direction M_x, M_y and M_z were calculated as follows:

$$M = \frac{d_m}{\sigma} \qquad (2)$$

where M is the slope of machine deflection (mm/kPa), d_m is the mechanical machine deflection (mm) and σ is the axial stress (kPa). The average mechanical machine deflections and the values of M in each direction during loading are presented in Figure 2(a). The measurements from the three LVDTs used to define these average mechanical machine deflections were nearly identical, indicating negligible bending of the aluminum face plates mounted to the space frame. The values of mechanical machine deflections can be subtracted from the measured deformation results from isothermal compression tests on soils during changes in stress. The z_1 face showed a softer response than the other directions, possibly because the bottom face in the z direction is a rigid plate. The application of anisotropic stresses in the z direction still resulted in linear elastic behavior, reflected in the same slope of the mechanical machine deflection curve.

It is critical to consider the deformation of the true-triaxial cell during heating and cooling in order to consider the effects of thermal expansion of the space frame when inferring the thermally induced volume change of soil specimens. After applying an isotropic stress state of 350 kPa to the aluminum cube (the same stress state used in the tests on the soils that will be discussed later), the system was heated from an ambient room temperature of 20 °C to a temperature of approximately 50 °C in three 10 °C intervals, then cooled back to ambient temperature in one stage. The change in temperature of the cell during heating is shown in Figure 2(b). The thermal machine deflections were calculated by subtracting the expected thermo-elastic deflection of the aluminum cube from the measured deflections. The LVDTs were used to measure the deflections of the five faces in the x, y and z directions during thermal cycling. The theoretical displacement of the aluminum cube in each direction was calculated as follows:

$$d_{T,al} = \alpha_{al} \times L_{al} \times \Delta T \quad (3)$$

where $d_{T,al}$ is the thermal displacement of the aluminum cube, α_{al} is the linear coefficient of thermal expansion of the aluminum (equal to 23×10^{-6} m/m°C), L_{al} is the initial length of aluminum cube and ΔT is the change in temperature applied during the test. The thermal machine deflections were calculated as the difference between the measured deflections from the LVDTs and the theoretical value of $d_{T,al}$ for a given change in temperature. Because the thermal machine deflections were found to be thermo-elastic, the slopes of the thermal machine deflection curves during heating H_x, H_y and H_z were calculated as follows:

$$H = d_T / \Delta T \tag{4}$$

where H is the slope of thermal machine deflection (mm/°C), d_T is the thermal machine deflection (mm) and ΔT is the change in temperature (°C). Although not shown here, Shanina (2015) found that the slopes of the thermal machine deflection curves during cooling were also relatively linear and similar to those during heating, so the slopes during heating were used to correct the thermal machine deflections through the entire test for simplicity.

Experimental Procedures

The first step in preparing the THM true-triaxial cell for a test is to saturate the HAE ceramic disk. As mentioned, this HAE ceramic disk is used to facilitate measurement of the negative water pressure in unsaturated soils using the tensiometer approach, to apply water pressures using the axis translation technique, and to measure potential outflow or inflow of water into the specimen during drained compression or heating. Accordingly, it is critical for the HAE ceramic disk to be saturated with water before beginning a test. The HAE ceramic disk was first placed into the recess in the rigid bottom platen of the THM true-triaxial cell in air-dry conditions. Then a bead of RTV silicon sealant was placed around the edge of the ceramic to provide a hydraulic seal that prevents short-circuiting of air around the edges of the HAE ceramic disk. After the silicon sealant cured, water was flushed through the channel beneath the ceramic disk. Next, a special pressure-saturation device was placed on top of the ceramic disk, which is described in detail by Shanina (2015). The device consists of a steel chamber with an O-ring seal at the base that is tightened onto the face of the rigid platen using three screws. After placement of the chamber atop the HAE ceramic disk, a vacuum of -70 kPa was applied to the base of the disk for

24 hours to de-air the ceramic. This chamber was then filled with de-aired water under a pressure of 70 kPa, and the same vacuum on the bottom side of the HAE ceramic disk was maintained. De-aired water was then permitted to flush downward through the HAE ceramic disk overnight. Water flow was oriented downward to avoid putting upward stresses on the seal between the hydro-thermal plate and the HAE disk. After this, the HAE ceramic was assumed to be water-saturated, and air breakthrough was not observed in any of the experiments.

Next, the compacted soil specimen was placed carefully on top of one of the flexible latex bladders outside of the THM cell so that the compaction lifts are perpendicular to the bladder face. The THM cell incorporates a tilting apparatus that can be used to facilitate placement of the soil specimen within the frame, which is described in detail by Mould (1983). After attaching the hydro-thermal face plate to the bottom of the frame (which is aligned with the z-axis), the frame was tilted 90° around the hinge-point. The specimen and the flexible bladder were then inserted into the THM cell from the bottom upward so that the z-face of the specimen, which is perpendicular to the compaction lifts, would be in contact with the hydro-thermal face plate. Then the frame was tilted back into the normal configuration.

Next, four thermocouples were installed into the system to measure the spatial distribution in temperature during the test. Two thermocouples were inserted into the compacted soil specimen, a third thermocouple was placed between the y_1 face of the compacted soil specimen and the bladder, and the fourth thermocouple was left outside to measure potential changes in the ambient room temperature. The ambient room temperatures were found to be relatively stable during testing and are reported by Shanina (2015). The thermocouples in the soil specimen were inserted using a needle so that they would measure the temperature near the mid-plane of the specimen and in between two lifts at similar distances from the lower hydro-thermal face plate and the upper z_1 bladder.

The bladders and mechanical loading plates were then assembled onto the true-triaxial cell frame. In the next step, fifteen LVDTs were placed on the top of the mechanical loading plates of the true triaxial cell. Each loading face contains three LVDTs, as three points are needed to define the orientation of a plane. Once the true-triaxial cell is assembled, the initial suction in the compacted, unsaturated silt was measured using the tensiometer approach described above.

A seating normal stress of 10 kPa was then applied to all of the bladders on the x- y- z-faces of the cubical soil specimen. This initial total stress was applied to ensure initial contact between the flexible latex bladders and the cubical specimen without causing significant deformations to the compacted specimen. The LVDT readings measured after equilibration under this initial seating stress were then zeroed to serve as a baseline reading from which to base further deformations of the specimen. After application of the seating stress, the initial value of suction measured within the specimen was applied using the axis translation technique. This involved increasing the total stress, pore air pressure, and pore water pressure in stages to maintain a constant suction within the specimen equal to the initial suction. The axis translation approach permits the pore water pressure applied to the bottom of the specimen to be positive, which minimizes the likelihood that the water will cavitate. The constant matric suction pressure was achieved by directly measuring the difference between the pore water and air pressures of the specimen (u_a-u_w = 20 kPa for S_r = 0.7 and u_a-u_w = 10 kPa for S_r = 0.8). The value of pore air pressure should be maintained greater than the value of pore water pressure, and both less than the value of total net stress. The isotropic and anisotropic loading-unloading tests were performed by increasing or decreasing the pressurized water through the bladders in increments and allowing the excess pore water pressure to dissipate.

Stresses were applied to the compacted soil specimens in order to reach three different anisotropic stress states represented by stress ratio K of 1.0, 0.7, and 0.5. In this study, it is assumed that the horizontal principal stresses are equal to the minor principal stress $\sigma_h = \sigma_x = \sigma_y = \sigma_3 = \sigma_2$), and that the vertical stress is the major principal stress ($\sigma_v = \sigma_z = \sigma_1$). As mentioned, the stress ratio is equal to the ratio of the minor principal stress to the major principal stress (K = $\sigma_3/\sigma_1 = \sigma_y/\sigma_z = \sigma_x/\sigma_z$). During mechanical loading, room-temperature water was used to pressurize the flexible bladders around the soil specimen. The specimen was first loaded isotropically up to 350 kPa in all cases, then the stress in the z direction was increased to reach the different target K values. This approach is different than that used by Coccia and McCartney (2012) and ensures that the mean stress never decreases during the tests and that the specimens remain normally consolidated during application of the anisotropic stress states.

After reaching the desired value of the anisotropy coefficient K, the soil specimens were heated in three stages then cooled in a single stage. This study focuses on the results from the heating stages of the experiments to facilitate comparison between the different conditions investigated, but the full set of test results can be found in Shanina (2015). The target rate of increasing water temperature was 0.5°C/hr to follow the approach of Uchaipichat and Khalili (2009). During heating, the water within the bladders was circulated through a pressurized reservoir that contains a heating coil. When the heating coil is activated, the water used to pressurize the flexible bladders heats up, and applies the same temperature to all sides of the cubical specimen. Because only one heating reservoir was available, and because the temperature at all six faces of the specimen should be the same, a copper circulation coil was placed inside the pressurized fluid within the bladder on the upper z-face. This approach permitted independent application of pressures to the z face bladder from the x and y face bladders, but uniform temperatures on all of the faces.

EXPERIMENTAL RESULTS

Six non-isothermal tests were conducted using the THM true-triaxial cell under constant suction conditions to characterize the effect of anisotropic stress states on the thermal volume changes of unsaturated soils. These tests were performed on compacted, cubical specimens of Bonny silt having different initial degrees of saturation and under different stress ratios K. The compaction conditions for these specimens are summarized in Table 1 along with the initial suction ψ_0, degree of saturation S_0, and temperature T_0. The tests performed on specimens with initial degrees of saturation of 0.7 and 0.8 complement tests on saturated specimens of compacted Bonny silt evaluated by Coccia and McCartney (2012). The name designations for each test along with the axial stresses applied to the specimens in the different tests are summarized in Table 2. The void ratios at the beginning of heating are also presented in this table, which are different from the initial values given in Table 1 due to the application of the isotropic stress state followed by the anisotropic stress state in some tests. The compression curves for these different tests are compared in Shanina (2015), who also presented time series of axial stress, axial displacement and temperature for the different tests. This study focuses on the synthesized average thermal axial strains measured in the different tests. It should be noted that because the heating tests were performed in drained conditions, the applied matric suction was constant during the tests. The outflow from the specimens were monitored during mechanical loading and heating, but negligible changes in degree of saturation were observed. This observation is consistent with the trends in degree of saturation during heating experiments on the same soil performed in a different experimental setup by Coccia and McCartney (2016a).

The thermal axial strains for the specimens with an initial degree of saturation of 0.7 having different initial stress ratios are shown in Figures 3(a), 3(b), and 3(c). The first observation from the data is that the thermal axial strains are contractile for all of the different stress ratios. This is consistent with the behavior of normally consolidated unsaturated silts observed by Uchaipichat and Khalili (2009) and Coccia and McCartney (2016a). The second observation is that with decreasing stress ratio, the thermal axial strain in the major stress direction (z) is observed to increase, while the thermal axial strains in the minor stress directions (x and y) are observed to decrease. For the isotropic test with K=1.0, the thermal axial strains in the x, y and z directions are similar, while for the anisotropic test with K=0.5, the thermal axial strain in the z direction is significant while it is negligible in the x and y directions. This observation is consistent with that of Coccia and McCartney (2012), who tested saturated specimens of Bonny silt. A comparison of the magnitude of thermal axial strains with those of Coccia and McCartney (2012) will be discussed later. Although not the focus of this study, Shanina (2015) reported the data from during cooling in these tests and observed irrecoverable, plastic deformations at the end of the test that would be expected when heating and cooling a normally-consolidated soil. A comparison between the thermal axial strains for the tests with an initial degree of saturation of 0.8 are shown in Figures 3(d), 3(e), and 3(f). The observations are consistent with those for the specimens with an initial degree of saturation of 0.7, although the magnitude of thermal axial strains are slightly smaller for the specimens with an initial degree of saturation of 0.8. Shanina (2015) also observed permanent deformations after cooling in these experiments.

The thermal volumetric strains for the three tests with an initial degree of saturation of 0.7 are shown in Figure 4(a). The thermal volumetric strain is equal to the sum of the three thermal axial strains measured in Figures 3(a), 3(b), and 3(c). The first observation is that the thermal volumetric strain for the three tests is relatively consistent despite the different stress ratios. This is consistent with the observation from Coccia and McCartney (2012) for saturated specimens of

Bonny silt. The thermal volumetric strains for the specimens with an initial degree of saturation of 0.8 are shown in Figure 4(b). The thermal volumetric strains are smaller than those for the specimens with an initial degree of saturation of 0.7, but a similar observation can be drawn that the thermal volumetric strains are relatively independent of the stress ratio.

ANALYSIS

Influence of Stress Induced Anisotropy

A synthesis of the thermal axial strains for the thermal axial strains at a change in temperature of 27 °C for all cases in the major and minor principal stress directions versus different K values are presented in Figure 5(a). Some of the tests were performed to higher temperatures, in which case, the results were linearly interpolated from the trend at the nearest measurement to estimate the thermal axial strain at 27 °C. Although the same conclusions drawn from Figure 3 can be drawn, an interesting observation is that the soils with an initial degree of saturation of 0.7 show greater thermal axial strains, with a greater difference between the thermal axial strains in the major and minor direction. The results are similar to those of Coccia and McCartney (2012), even though their anisotropic stress states were reached by unloading the specimen in the minor stress direction and thus incorporating an overconsolidation effect. Instead, the results in this study may indicate that greater thermal strains occur in the direction that has accumulated more plastic strains due to mechanical loading. This hypothesis is consistent with the thermally accelerated secondary compression model proposed by Coccia and McCartney (2016b).

A synthesis of the volumetric strain versus the stress ratio for the specimens having initial degrees of saturation of 0.7 and 0.8 is shown in Figure 5(b) for a change in temperature of 27 °C. Although there is some slight fluctuation in the curves with K, the thermal volumetric strain is not as sensitive to the value of K as the thermal axial strain. Further, it is clear that the specimens with an initial degree of saturation of 0.8 have a consistently lower thermal volume change that those with an initial degree of saturation of 0.7.

As Coccia and McCartney (2012) evaluated Bonny silt under saturated conditions, their results were compared to those of this study in terms of the thermal volumetric strain in Figure 6. It is not possible to fairly compare the thermal axial strains because Coccia and McCartney (2012) applied the major and minor principal stresses in the x- and y-directions, applied the anisotropic stress state by unloading, and did not control the principal stress in the z-direction. Nonetheless, the comparison in Figure 6 permits an approximate assessment of the influence of the initial degree of saturation on the thermal volumetric strain. Although there is some scatter, the thermal volumetric strains for the specimens with an initial degree of saturation of 1.0 are slightly lower on average than those with an initial degree of saturation of 0.8, reflecting that a greater amount of thermal collapse may occur in the dryer soils under normally consolidated conditions. Coccia and McCartney (2016a) observed a greater amount of contraction with decreasing degree of saturation up to a certain point (S_0 of 0.56), but then observed a lower amount of contraction.

Model for Anisotropy Effects

The thermal volumetric strain for the cubical soil specimen can be calculated from the axial thermal strains as follows:

$$\varepsilon_{vT} = \varepsilon_{xT} + \varepsilon_{yT} + \varepsilon_{zT} + \left(\varepsilon_{xT} \times \varepsilon_{yT} + \varepsilon_{xT} \times \varepsilon_{zT} + \varepsilon_{yT} \times \varepsilon_{zT}\right) + \varepsilon_{xT} \times \varepsilon_{yT} \times \varepsilon_{zT} \quad (5)$$

where ε_{vT} is the total thermal volumetric strain and $\varepsilon_{xT,}$ ε_{yT}, ε_{zT} are the thermal axial strains in the x, y and z directions. This equation can be simplified by assuming that the higher order terms are negligible because the thermal axial strains are very small. Accordingly, the thermal volumetric strain can be expressed as follows:

$$\varepsilon_{vT} = \varepsilon_{xT} + \varepsilon_{yT} + \varepsilon_{zT} \qquad (6)$$

In the true-triaxial experiment, the three orthogonal thermal axial strains are assumed to be equal to the principal strains. Most well-established thermo-elasto-plastic models use an isotropic thermal yield surface (Cui et al. 2000; Abuel-Naga et al. 2009), and focus on prediction of the thermal volumetric strain rather than the individual axial strains. Although a thermo-elasto-plastic model could be developed that considers thermal yielding individually in each direction, a simpler approach was followed in this study. Specifically, using the fact that the volumetric thermal strain is not sensitive to the stress ratio K [i.e., Figure 6(b)], the volumetric strains predicted from the established isotropic thermo-elasto-plastic models can be partitioned using an empirical relationship based on the results presented in this study. Further, an empirical relationship can also be incorporated to account for the influence of the initial degree of saturation on the parameters of the established thermo-elasto-plastic model.

In order to do this, an approach similar to that proposed by Coccia (2011) was used to define an empirical relationship between the thermal axial strains in the major and minor principal stress directions and the stress ratio. The thermal axial strain ratio (Ω) was defined to relate the thermal axial strains in the minor principal stress directions (x and y) and the major principal stress direction (z), as follows:

$$\Omega = \varepsilon_{yT} / \varepsilon_{zT} \qquad (7)$$

The trend in Ω observed in the current study for Bonny silt under different stress ratios (K = σ_y/σ_z) and different degrees of saturation is shown in Figure 7. This figure also includes the data from Coccia (2011). The first observation is that the trend between W and K does not appear to be sensitive to the degree of saturation, except for a strongly negative value of Ω for the saturated specimen under the lowest K value of 0.5. This point was assumed to be an outlier in the development of a best fit power law relationship, which is shown in Figure 7. Although Coccia (2011) used a different form of equation to represent the nonlinear decreasing trend in Ω, the additional results presented in this study better establish the trend between Ω and K. The relationship for Ω is only extended to a value of K = 0.325, as this is the minimum value of K corresponding to shear failure for this soil (corresponding to a friction angle of 33°). The experimental and best-fit values of Ω for the specimens with K=1 are not equal to 1.0 even though this corresponds to an isotropic stress state because of inherent anisotropy effects associated with how the specimen was compacted with lifts perpendicular to the z direction.

Combining Equations 6 and 7 leads to the following relationship:

$$\varepsilon_{zT} = \frac{\varepsilon_{vT}}{(2\Omega + 1)} \tag{8}$$

which can be written in differential form as follows:

$$d\varepsilon_{zT} = \frac{d\varepsilon_{vT}}{(2\Omega + 1)} \tag{9}$$

The differential form of the thermal axial strain in the y or x directions can be calculated similarly, as follows:

$$d\varepsilon_{yT} = \frac{d\varepsilon_{vT}\Omega}{(2\Omega + 1)} \tag{10}$$

By incorporating combined incremental forms of the elastic and plastic volumetric strains from the constitutive model of Cui et al. (2000), Equation 9 can be rewritten as follows:

$$d\varepsilon_{zT} = \frac{1}{(2\Omega + 1)}\left[\alpha_2 dT + \alpha_p\left(\exp\left(\alpha_p \Delta T\right) - a\right)dT\right] \tag{11}$$

while Equation 10 can be rewritten as follows:

$$d\varepsilon_{yT} = \frac{\Omega}{(2\Omega+1)}\left[\alpha_2 dT + \alpha_p\left(\exp\left(\alpha_p \Delta T\right) - a\right)dT\right] \tag{12}$$

where α_2 is a constant parameter representing the drained coefficient of thermo-elastic expansion of a soil obtained from a cooling test performed at a slow rate, α_p is a constant parameter that depends on the overconsolidation ratio, *a* is a constant shape parameter representing the evolution of the plastic thermal volumetric strain with temperature, ΔT is the total change in temperature (°C) from a reference temperature, and dT is the increment in temperature from one step to another (°C). The value of α_2 was calculated to be approximately -0.0007/°C from cooling tests on Bonny silt reported by Shanina (2015). Cui et al. (2000) assumed that $\alpha_p = -\alpha_2/(1-a)$ for normally consolidated soils. In this case, Equation 11 can be rewritten as follows:

$$d\varepsilon_{zT} = \frac{1}{(2\Omega+1)}\left[\alpha_2 dT - \frac{\alpha_2}{1-a}\left(\exp\left(-\frac{\alpha_2}{1-a}\Delta T\right) - a\right)dT\right] \tag{13}$$

and Equation 12 can be rewritten as follows:

$$d\varepsilon_{yT} = \frac{\Omega}{(2\Omega+1)}\left[\alpha_2 dT - \frac{\alpha_2}{1-a}\left(\exp\left(-\frac{\alpha_2}{1-a}\Delta T\right) - a\right)dT\right] \tag{14}$$

The incremental form of the model of Cui et al. (2000) was used in this study so the combined effects of elastic thermal expansion and plastic thermal contraction expected during heating of normally consolidated soils could be superimposed atop each other. This assumes that some elastic thermal expansion will always occur during heating. The advantage of this approach is that the elastic thermal expansion can be separated from the overall observed thermal contraction in the experiments, which permits a more accurate definition of the model parameter *a*.

In addition to the influence of the anisotropic stress state, the influence of unsaturated conditions observed in Figure 6(a) needs to be incorporated into the prediction of the thermal volumetric strain. The thermal axial strain for unsaturated soils was estimated by assuming that the α_p parameter in the model of Cui et al. (2000) is also a function of the degree of saturation. Specifically, Equation 14 was updated by modifying the definition of α_p assumed by Cui et al. (2000) to include the product of a constant parameter *b* and the effective saturation at the start of heating ($S_{e,0} = \frac{S_0 - S_{res}}{1 - S_{res}}$, where S_0 is the initial degree of saturation, and S_{res} is the residual degree of saturation) in the denominator, as follows:

$$d\varepsilon_{zT} = \frac{1}{(2\Omega+1)}\left[\alpha_2 dT - \frac{\alpha_2}{bS_{e,0}(1-a)}\left(\exp\left(-\frac{\alpha_2}{bS_{e,0}(1-a)}\Delta T\right) - a\right)dT\right] \qquad (16)$$

Similarly Equation 15 can be modified as follows:

$$d\varepsilon_{yT} = \frac{\Omega}{(2\Omega+1)}\left[\alpha_2 dT - \frac{\alpha_2}{bS_{e,0}(1-a)}\left(\exp\left(-\frac{\alpha_2}{bS_{e,0}(1-a)}\Delta T\right) - a\right)dT\right] \qquad (17)$$

This modified form of the Cui et al. (2000) model assumes that the initial effective saturation affects the thermal axial strain, and that any potential changes in degree of saturation during heating do not have a major effect on the value of the thermal axial strain. As no change in degree of saturation was observed for this soil during heating by Shanina (2015) and Coccia and McCartney (2016a), this assumption is reasonable. However, this is a topic that may need further study for other soils.

Comparisons of the measured and simulated thermal axial strains for the specimens with an initial degree of saturation of 0.7 are shown in Figures 8(a), 8(b), and 8(c) for K values of 1.0, 0.7, and 0.5, respectively. The differential thermal axial strains from Equations 16 and 17 were integrated to define the total thermal axial strains. A good fit is observed between the model and experimental results for a value of *a* equal to 0.323. Similarly, comparisons of the measured and simulated thermal axial strains for the specimens with an initial degree of saturation of 0.8 are shown in Figures 8(d), 8(e), and 8(f) for K values of 1.0, 0.7, and 0.5, respectively. A value of *b* equal to 1.95 was observed to provide a good fit to this data, as well as to the saturated data of Coccia and McCartney (2012) that is not shown here for brevity but is shown in Shanina (2015). A plot of the thermal volumetric strains for the same specimens with degrees of saturation of 0.7 and 0.8 along with the model simulations are shown in Figures 9(a) and 9(b), respectively, and a good fit is also observed to the data. Although this model is simple and empirical, it shows how an established isotropic thermo-elasto-plastic model such as that of Cui et al. (2000) can be extended to predict the thermal axial strains in principal stress directions for different anisotropic stress states. Nonetheless, the role of unsaturated conditions through the *b* parameter needs to be further verified through testing of other soils over a wider range of suction.

DISCUSSION

The results from this study confirm the importance of considering the influence of anisotropic stress states on the thermal volume change of soils. Natural soils typically have an inherent anisotropy, corresponding to at-rest or K_0 conditions. As K_0 is typically less than 1 in natural soil deposits, this means that the vertical stress is greater than the horizontal stress. If the soil under this stress state is heated, then different magnitudes of thermal axial strains are expected. The value of K may change more significantly in the case of the installation of an energy pile, which typically involves excavation and a lower K value that is closer to active earth pressure conditions.

When the soil surrounding an energy pile changes in temperature, potentially irreversible soil volume changes in the soil may occur. If the soil is overconsolidated, it is likely that the soil will expand in both the vertical and horizontal directions elastically. In this case, the thermal volume changes are not expected to be significant. More significant changes are expected to occur if the soil is closer to normally consolidated conditions in the vertical direction, in which case contraction would be expected in both the vertical and horizontal directions as observed in this study. The contractile thermal axial strain in the horizontal direction may lead to a reduction in the lateral stress distribution along the energy foundation, and may lead to relative movement due to the existing mechanical stress being transferred from the foundation to the surrounding soil. Further, the thermal axial strain the vertical direction will be greater than that in the horizontal direction, and may lead to dragdown forces on the energy pile that are superimposed atop any mechanical or thermo-mechanical strains that are predicted to occur using a load-transfer analysis such as that of Knellwolf et al. (2011). Nonetheless, for the soil that was evaluated in this study, the magnitudes of thermal axial strain are all less than 1%, which is relatively small. The only likelihood that these thermal axial strains will affect the performance of the foundation would be if it were heavily loaded close to its ultimate capacity.

The isotropic thermo-elasto-plastic model of Cui et al. (2000) was adapted in this study to empirically consider the effects of anisotropic stress states as well as to include the influence of unsaturated conditions. This model is simple to use in the fact that it can predict the thermal axial strains for a given change in soil temperature from the value of predicted thermal volumetric strain from an established isotropic thermo-elasto-plastic model. In this case, a finite element model may be used to predict the change in temperature of the soil as a function of space and time using a transient conduction analysis. After this, the model can be used to estimate the thermal axial strains in a de-coupled manner (assuming the thermal axial strains are just due to changes in temperature and are independent of the mechanical stresses). These strains would have to be superimposed on top of a mechanical stress-strain analysis to see if mechanical changes in pile behavior would occur.

Regarding the role of unsaturated conditions, this study indicates that this is an important variable to consider. Different trends in the magnitude of thermal volume change were observed for the soil tested in this study than in previous studies such as Uchaipichat and Khalili (2009). Nonetheless, the tests in this previous study underwent undrained heating and cooling cycles and several different loading and unloading cycles before heating, which may have had a cumulative effect on the results. A mechanism for the increasing trend in thermal volume change with decreasing thermal volume change was not explicitly proposed in this study due to the relatively limited number of specimens with different degrees of saturation, although this behavior may be due to the collapse of air voids during drained heating, or to thermally accelerated creep after application of plastic strains during mechanical loading (Coccia and McCartney 2016b).

CONCLUSIONS

This study involved the development of a thermo-hydro-mechanical true triaxial cell which is capable of measuring the thermal deformations of unsaturated soils under various anisotropic stress states. In addition to calibrating and characterizing the response of the true-triaxial cell, several experiments were performed on specimens having different minor to major stress ratios and to different initial degrees of saturation. The specimens were all loaded to normally consolidated conditions isotropically before application of the different anisotropic stress states. The major conclusions that can be drawn from the evaluation of the results from these test include:

- The thermally-induced axial and volumetric strains during heating for all tests on the normally consolidated, compacted Bonny silt specimens showed contractile behavior, regardless of the stress state and the initial degree of saturation.
- The plastic thermal contraction trends in the volumetric strains observed in this study are consistent with those published in the literature for normally consolidated soils.
- With decreasing values of stress ratio K, the thermal axial strains in the major principal stress direction (z) were observed to increase, while the thermal axial strains in the minor principal stress directions (x, y) are observed to decrease. However, for isotropic conditions (K = 1), the thermal axial strains were slightly greater in the x and y directions than in the z directions even though the stresses were the same. This was attributed to the effects of inherent anisotropy associated with how the specimens were formed by compacted.
- Consistent with observations from tests on saturated Bonny silt specimens reported by Coccia and McCartney (2012), the thermal volumetric strains were relatively similar regardless of the stress ratio K. This indicates that anisotropic stress states may lead to different thermal deformations in different directions but the same overall volumetric response.
- Specimens with a lower initial degree of saturation were observed to show greater thermal axial strains. The data reported by Coccia and McCartney (2012) for saturated specimens of the same soil are consistent with these trends in that greater thermal axial strains are measured for the unsaturated specimens than the saturated specimens. The trends with degree of saturation differed from that of Uchaipichat and Khalili (2009), who observed a very slight decrease in thermal volume strain with decreasing degree of saturation. However, their tests

involved application of multiple loading stages and undrained heating and cooling cycles before the drained heating tests.

- The isotropic elasto-plastic model of Cui et al. (2000) for saturated soils was combined with empirical relationships to account for the effects of anisotropic stress states and the initial degree of saturation. An empirical relationship between the ratio of thermal axial strains in the major and minor principal stress directions and the stress ratio was developed that appears to be insensitive to the degree of saturation. This relationship also incorporated the effects of inherent anisotropy in the compacted specimens. The adapted thermo-elasto-plastic model is capable of considering the effects of anisotropic stress states as well as the influence of unsaturated conditions for Bonny silt, although further confirmation is required for other soils over a wider range of unsaturated conditions.

ACKNOWLEDGMENTS

Funding from Libyan government and NSF CMMI 1054190 is greatly appreciated. The opinions in this paper are those of the authors alone.

APPENDIX I. REFERENCES

Abuel-Naga, H. M., Bergado, D. T., Bouazza, A. and Ramana, G. V. (2007). "Volume change behavior of saturated clays under drained heating conditions: experimental results and constitutive modeling." Canadian Geotechnical Journal. 44(8), 942-956.

Abuel-Naga, H.M., Bergado, D.T., Bouazza, A., and Pender, M. (2009). "Thermomechanical model for saturated clays." Géotechnique, 59(3), 273–278.

Adam, D. and Markiewicz, R. (2009). "Energy from earth-coupled structures, foundations, tunnels and sewers," Géotechnique. 59(3), 229–236.

Alsherif, N.A. and McCartney, J.S. (2015). “Nonisothermal behavior of compacted silt at low degrees of saturation.” Géotechnique. 65(9), 703-716. DOI: 10.1680/geot./14-P-049.

Alsherif, N. and McCartney, J.S. (2016). “Yielding of silt at high temperature and suction magnitudes.” Geotechnical and Geological Engineering. 1-14. 10.1007/s10706-015-9961-x.

Baldi, G., Hueckel, T. and Pelegrini, R. (1988). “Thermal volume changes of the mineral-water system in low-porosity clay soils.” Canadian Geotechnical Journal. 25, 807-825.

Brandl, H. (2006). “Energy foundations and other thermo-active ground structures.” Géotechnique. 56(2), 81-122.

Burghignoli A., Desideri A., and Miliziano S. (2000). “A laboratory study on the thermomechanical behaviour of clayey soils.” Canadian Geotechnical Journal. 37: 764-780.

Campanella, R.G. and Mitchell, J.K. (1968). “Influence of temperature variations on soil behavior.” Journal of the Soil Mechanics and Foundation Engineering Division. 94(3), 709–734.

Cekerevac, C. and Laloui, L. (2004). “Experimental study of thermal effects on the mechanical behaviour of a clay.” International Journal of Numerical and Analytical Methods in Geomechanics. 28(3), 209–228.

Coccia, C.J.R. (2011). Impact of Stress-Induced Anisotropy on Thermal Volume Change in Saturated Soils. MS Thesis. University of Colorado Boulder. 127 pg.

Coccia, C.J.R. and McCartney, J.S. (2012). “A thermo-hydro-mechanical true triaxial cell for evaluation of the impact of anisotropy on thermally induced volume changes in soils.” Geotechnical Testing Journal. 35(2), 227-237.

Coccia, C.J.R. and McCartney, J.S. (2016a). “Thermal volume change of poorly draining soils I: Critical assessment of volume change mechanisms.” Computers and Geotechnics. 80(December), 26-40.

Coccia, C.J.R. and McCartney, J.S. (2016b). “Thermal volume change of poorly draining soils II: Constitutive modelling.” Computers and Geotechnics. 80(December), 16-25.

Cui, Y.J., Sultan, N., and Delage, P. (2000). “A thermomechanical model for saturated clays.” Canadian Geotechnical Journal, 37(3), 607–620.

Delage, P., Sultan, N., and Cui, Y.J. (2000). “The thermal consolidation of Boom Clay,” Canadian Geotechnical Journal. 37, 343-354.

Demars, K.R., and Charles, R.D. (1982). “Soil volume changes induced by temperature cycling.” Canadian Geotechnical Journal. 19, 188–194.

Francois, B. Salager, S., El Youssoufi, M.S., Ubals Picanyoul, D., Laloui, L., and Saix, C. (2007). “Compression tests on a sandy silt at different suction and temperature levels.” GSP 157: Computer Applications in Geotechnical Engineering. 1-10.

Hilf, J.W. (1956). An Investigation of Pore-water Pressure in Compacted Cohesive Soils. Technical Memo No.654, United States Bureau of Reclamation, Denver.

Hoyos, L.R. and Macari, E.J. (2001). “Development of a stress/suction-controlled true triaxial testing device for unsaturated soils.” Geotechnical Testing Journal. 24(1), 5 13.

Hoyos, L. R., Laikram, A., and Puppala, A. J. (2008). “A novel suction controlled true triaxial apparatus for unsaturated soils.” Chapter 5, Unsaturated Soils: Advances in Geo-engineering. D.G. Toll, C.E. Augarde, D. Gallipoli and S.J. Wheeler, eds., CRC, London, 83–88.

Hoyos, L.R., Pērez-Ruiz, D.D. and Puppala, A.J. (2012). ”Refined true triaxial apparatus for testing unsaturated soil under suction controlled stress path.” International Journal of Geomechanics. 12(3), 281–291.

Hueckel, T. and Baldi, M. (1990). “Thermoplasticity of saturated clays: experimental constitutive study.” Journal of Geotechnical Engineering. 116(12), 1778–1796.

Hueckel, T. and Borsetto, M. (1990). “Thermoplasticity of saturated soils and shales: Constitutive equations.” Journal of Geotechnical Engineering. 116(12), 1765-1777.

Hueckel, T. and Pellegrini, R. (1996). “A note on thermomechanical anisotropy of clays,” Eng. Geo. (Amsterdam). 41, 171-180.

Knellwolf, C., Peron, H., and Laloui, L. (2011). “Geotechnical analysis of heat exchanger piles.” ASCE Journal of Geotechnical and Geoenvironmental Engineering. 137(12), 890-902.

Ko, H.Y., and Scott, R.F. (1967). “A new soil testing apparatus.” Géotechnique. 17(1), 40-57.

Laloui, L. and Cekerevac, C. (2003). “Thermo-plasticity of clays: an isotropic yield mechanism.” Computers and Geotechnics. 30(8), 649–660.

Laloui, L., Nuth, M., and Vulliet, L. (2006). “Experimental and numerical investigations of the behavior of a heat exchanger pile.” International Journal of Numerical and Analytical Methods in Geomechanics. 30(8), 763-781.

McCartney, J.S. (2011). “Engineering performance of energy foundations.” Invited Theme Paper. 2011 PanAm CGS Geotechnical Conference. Can. Geotech. Society. Toronto. Oct. 2-6. 1-14.

McCartney, J.S. (2012). “Issues involved in using temperature to improve the mechanical behavior of unsaturated soils.” Unsaturated Soils, Theory and Practice 2011: Proceedings of 5th Asia-Pacific Unsaturated Soils Conference. A. Jotisankasa, A. Sawangsuriya, S. Soralump and W. Mairaing, eds. Kasetsaert University, Thailand. pp. 509-514.

Mould, J.C. (1983), Stress Induced Anisotropy in Sand and the Evaluation of a Multi-Surface Elasto-Plastic Material Model. Ph.D. Thesis, Univ. of Colorado.

Murphy, K.D. and McCartney, J.S. (2015). “Seasonal response of energy foundations during building operation.” Geotechnical and Geological Engineering. 33(2), 343-356.

Murphy, K.D., McCartney, J.S., and Henry, K.S. (2015). “Thermo-mechanical response tests on energy foundations with different heat exchanger configurations.” Acta Geotechnica. 10(2), 179-195.

Romero, E., Gens, A., Lloret, A. (2003). “Suction effects on a compacted clay under non-isothermal conditions.” Géotechnique. 53(1), 65–81.

Salager, S., El Youssoufi, M.S., and Saix, C. (2007). “Influence of temperature on the water retention curve of soils: Modelling and experiments.” Experimental Unsaturated Soil Mechanics. Schanz, T. ed. pp. 251-258.

Shanina, M. (2015). Impact of Anisotropy on the Thermal Volume Change of Unsaturated Silt using a Thermo-Hydro-Mechanical True-Triaxial Cell. Ph.D. Thesis, U. of Colorado Boulder.

Sultan, N., Delage, P. and Cui, Y.J. (2002). “Temperature effects on the volume change behavior of boom clay.” Engineering Geology. 64, 135-145.

Tang, A.M., Cui, Y.J. and Barnel, N. (2008). “Thermo-mechanical behavior of a compacted swelling clay.” Géotechnique. 58(1), 45-54.

Takata, S. (2000). Upgrade of a Large Scale True Triaxial Apparatus for Shear Strength Characterization.” Master Thesis, University of Colorado.

Towhata, I., Kuntiwattanakul, P., Seko, I. and Ohishi, K. (1993). “Volume change of clays induced by heating as observed in consolidation tests.” Soils and Foundations. 33(4), 170-183.

Uchaipichat, A. and Khalili, N. (2009). “Experimental investigation of thermo-hydro-mechanical behaviour of unsaturated silt.” Géotechnique, 59(4), 339-353.

Vega, A. and McCartney, J.S. (2015). “Cyclic heating effects on thermal volume change of silt.” Environmental Geotechnics. 2(5), 257-268.

LIST OF TABLE AND FIGURE CAPTIONS

Table 1: Initial conditions of the soil specimens evaluated in this study

Table 2: Applied stresses in the tests having different stress ratios K

Fig. 1: Schematic of the modified THM true-triaxial cell: (a) Hydro-thermal bottom face plate and side bladders filled by pressurized hot water with soil specimen; (b) Top view of the THM cell showing the hydro-thermal control plate

Fig. 2: Machine deflections for the true-triaxial cell: (a) Mechanical; (b) Thermal

Fig. 3: Thermal axial strains for the specimens with different initial degrees of saturation and stress ratios: (a) S = 0.7, K = 1.0; (b) S = 0.7, K = 0.7; (c) S = 0.7, K = 0.5; (d) S = 0.8, K = 1.0; (e) S = 0.8, K = 0.7; (f) S = 0.8, K = 0.5

Fig. 4: Thermal volumetric strains for the specimens different stress ratios: (a) S = 0.8; (b) S = 0.7

Fig. 5: Summary of equilibrium points for tests under different initial degrees of saturation and stress ratios at a change in temperature of 27 °C: (a) Thermal axial strains in the major and minor principal directions; (b) Thermal volumetric strains

Fig. 6: Thermal volumetric strains from this study compared with those for saturated specimens from Coccia and McCartney (2012)

Fig. 7: Thermal axial strain ratio as a function of stress ratio for Bonny silt with different degrees of saturation proposed in this study

Fig. 8: Comparison between predicted and observed thermal axial strains for the specimens with: (a) S = 0.7, K = 1.0; (b) S = 0.7, K = 0.7; (c) S = 0.7, K = 0.5; (d) S = 0.8, K = 1.0; (e) S = 0.8, K = 0.7; (f) S = 0.8, K = 0.5

Fig. 9: Comparison between predicted and observed thermal volumetric strains for specimens with: (a) S = 0.7 and different stress ratios; (b) S = 0.8 and different stress ratios

Table 1: Initial conditions of the soil specimens evaluated in this study

Test	Stress ratio, K = σ_y/σ_z	Gravimetric water content, w (%)	Dry density, ρ_d (kg/m^3)	Initial void ratio	Initial degree of saturation, S_0	Measured initial suction, ψ_0 (kPa)	Initial temperature*, T_0 (°C)
K1.0-S0.7	1.00	16.08	1650	0.594	0.712	20.0	19.70
K0.7-S0.7	0.70	15.32	1661	0.584	0.690	20.0	19.21
K0.5-S0.7	0.50	15.99	1651	0.593	0.709	20.0	19.25
K1.0-S0.8	1.00	18.52	1644	0.600	0.812	10.0	19.24
K0.7-S0.8	0.70	18.39	1646	0.598	0.808	10.0	19.10
K0.5-S0.8	0.50	17.70	1655	0.589	0.790	10.0	19.20

*Note: The initial temperature is the highest temperature previously experienced by the soil

Table 2: Applied stresses in the tests having different stress ratios K

Test	Stress ratio, K = σ_y'/σ_z'	Stresses at the start of heating				Void ratio at the start of heating
		σ_x' (kPa)	σ_y' (kPa)	σ_z' (kPa)	p' (kPa)	
K1.0-S0.7	1.0	274	274	274	274	0.580
K0.7-S0.7	0.7	274	274	424	324	0.571
K0.5-S0.7	0.5	274	274	624	391	0.567
K1.0-S0.8	1.0	268	268	268	268	0.590
K0.7-S0.8	0.7	268	268	418	318	0.577
K0.5-S0.8	0.5	268	268	618	385	0.571

Figure 1
Click here to download high resolution image

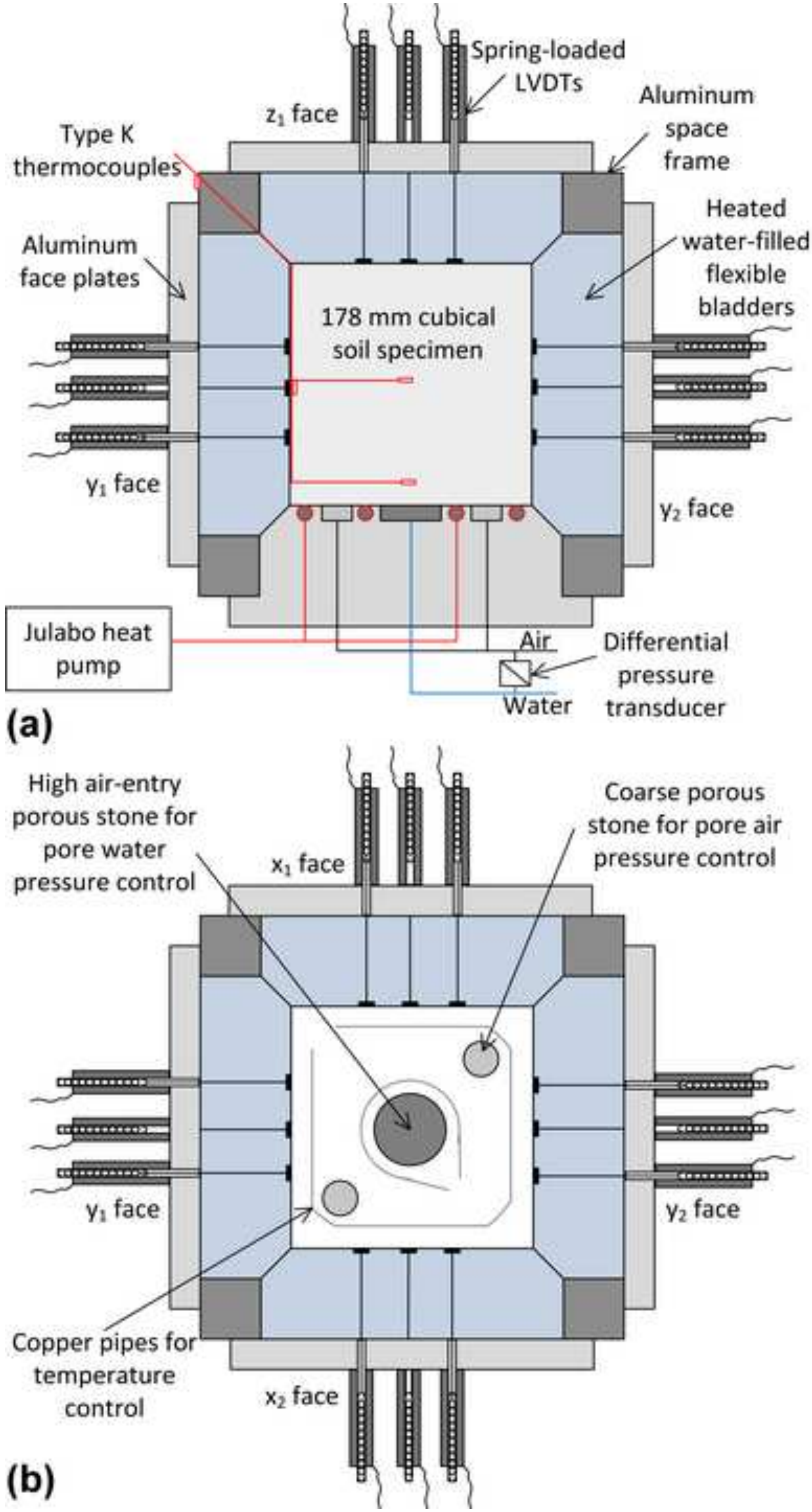

Figure 2

Click here to download high resolution image

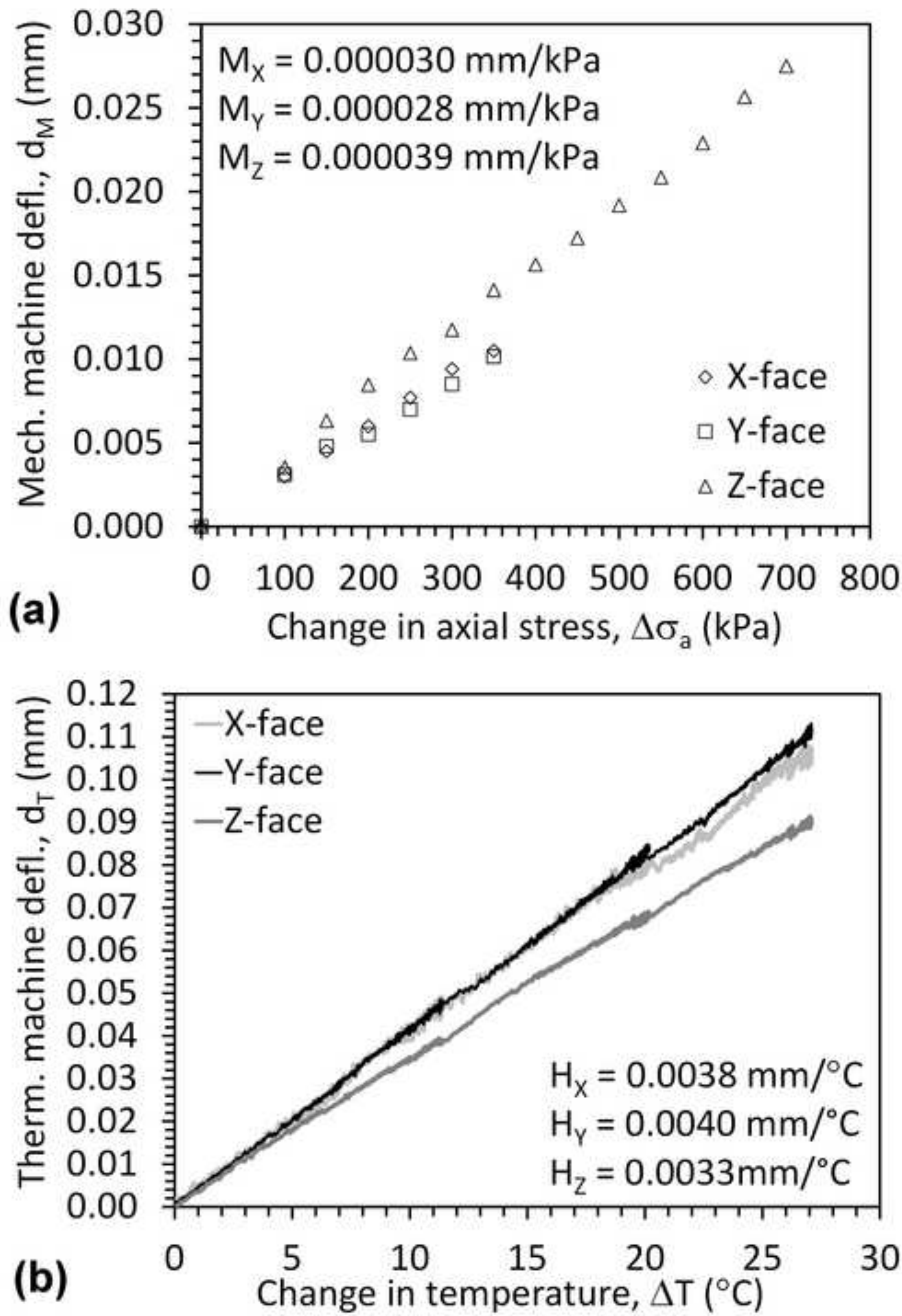

Figure 3
Click here to download high resolution image

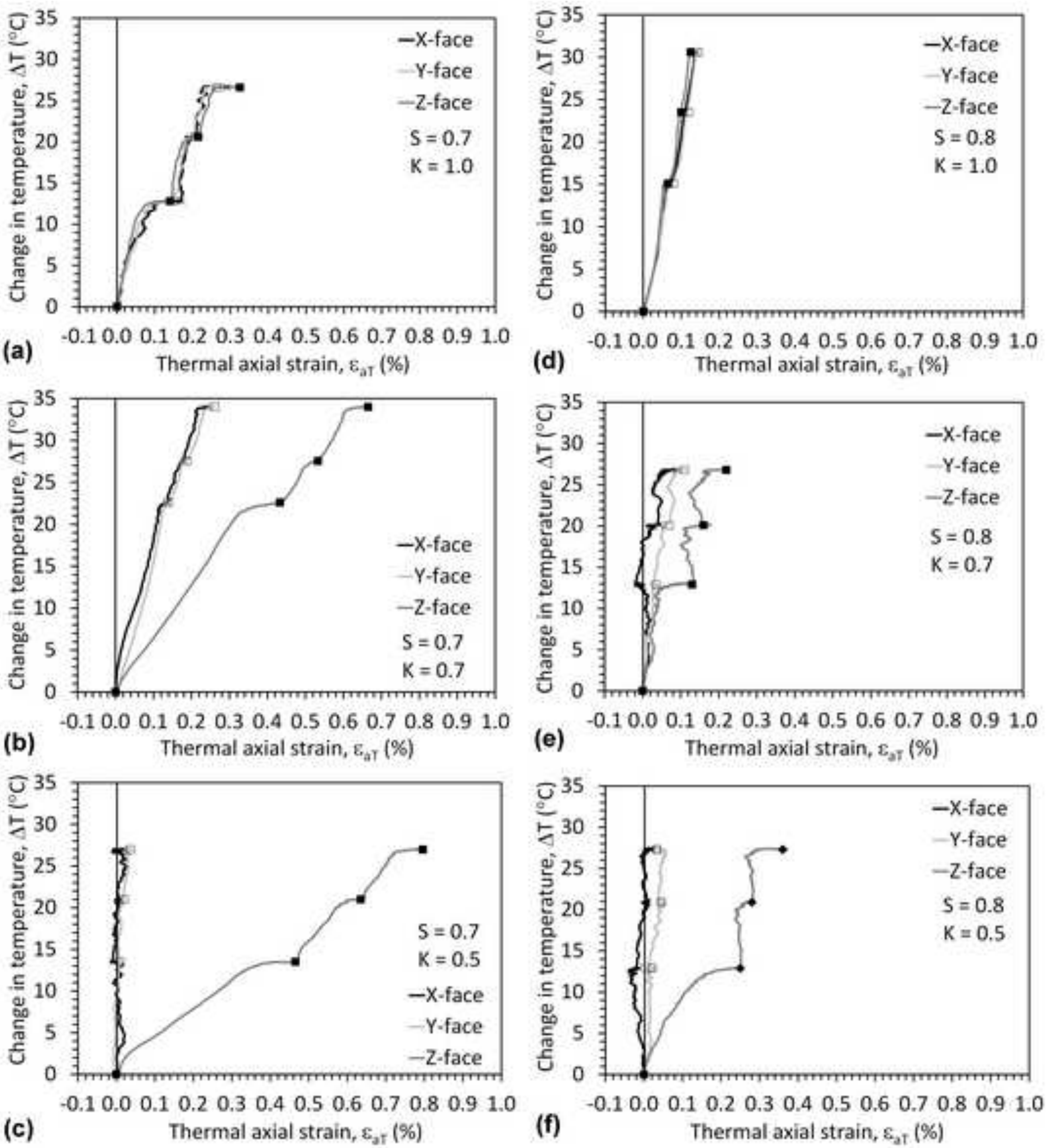

Figure 4

Click here to download high resolution image

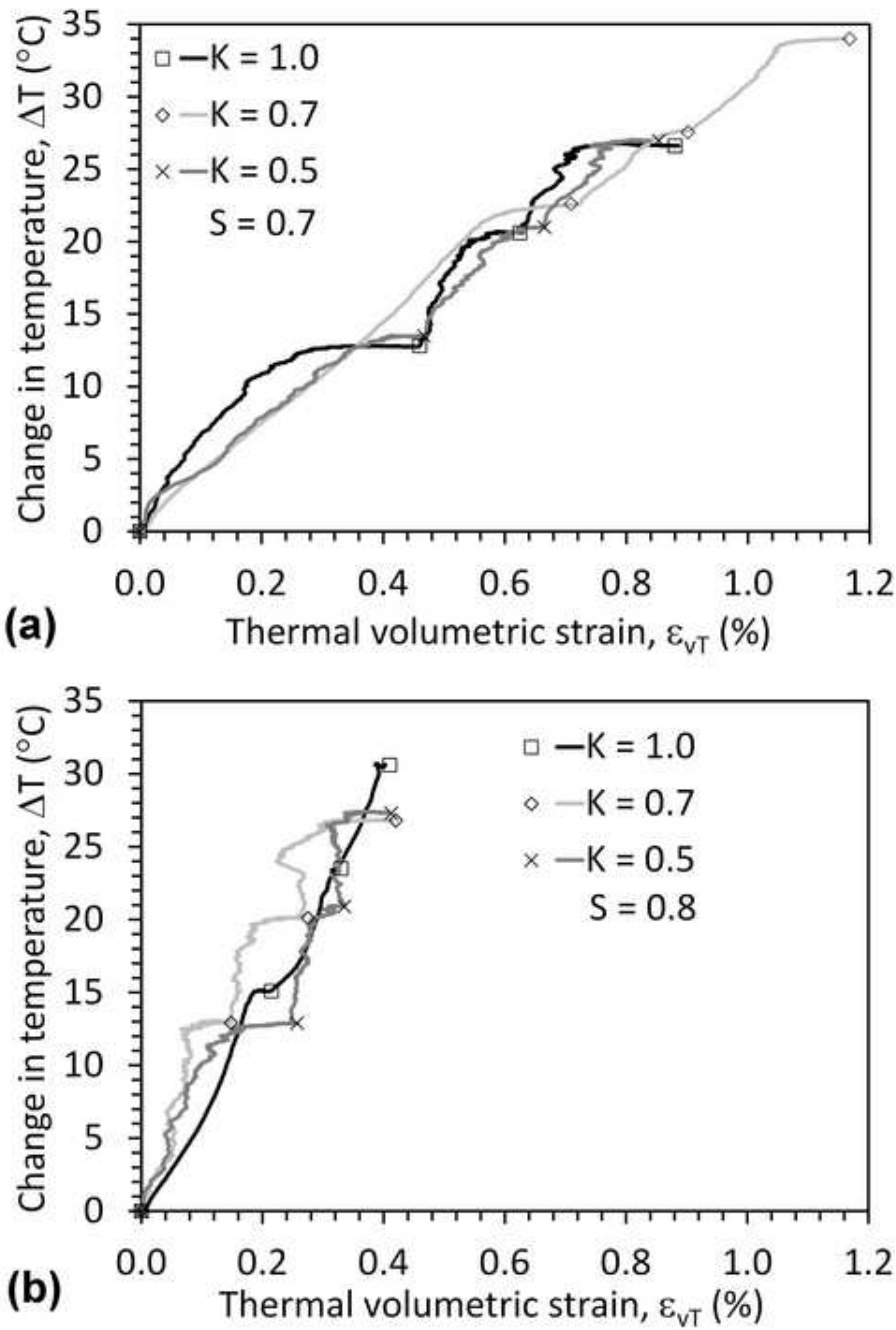

Figure 5
Click here to download high resolution image

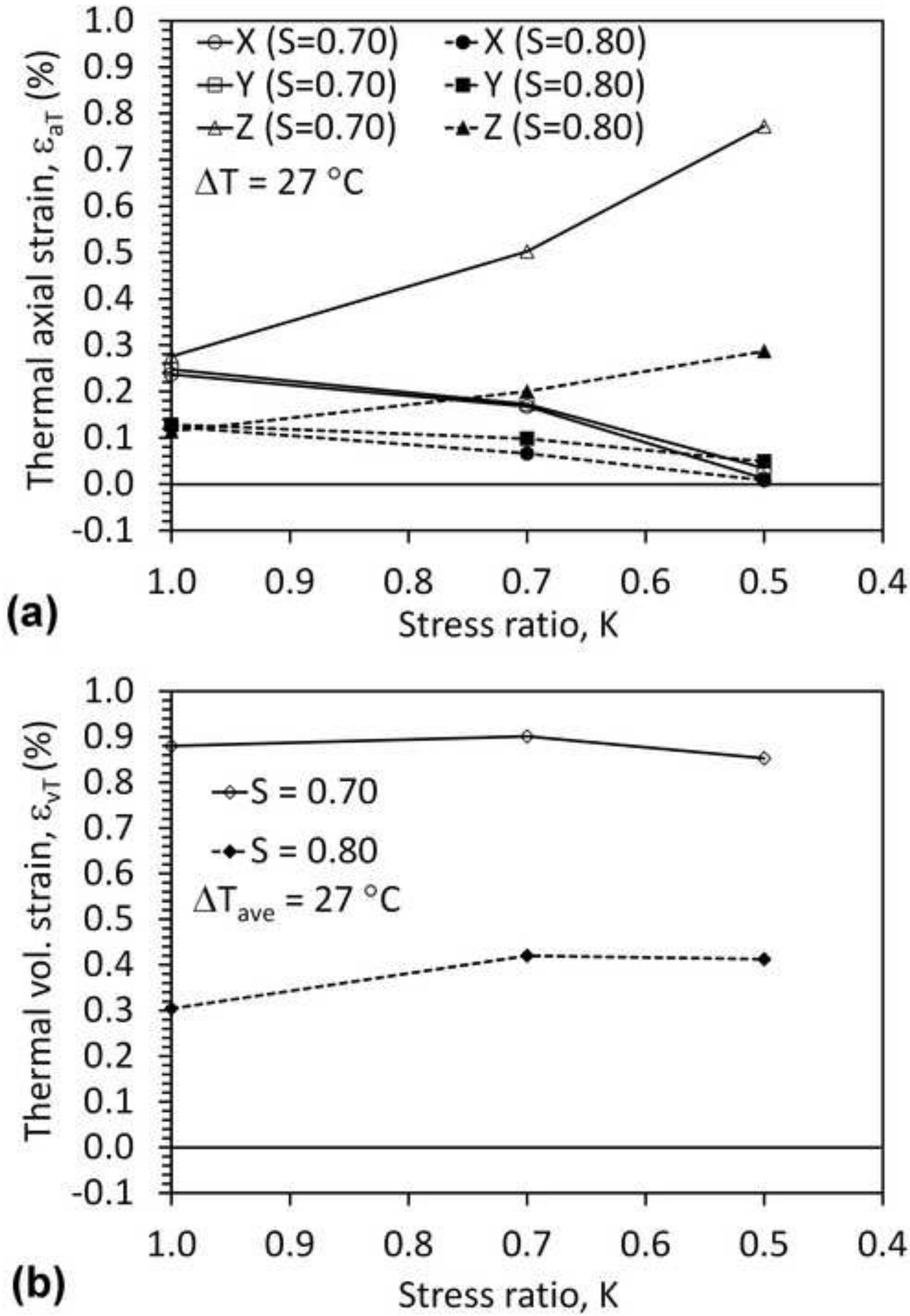

Figure 6
Click here to download high resolution image

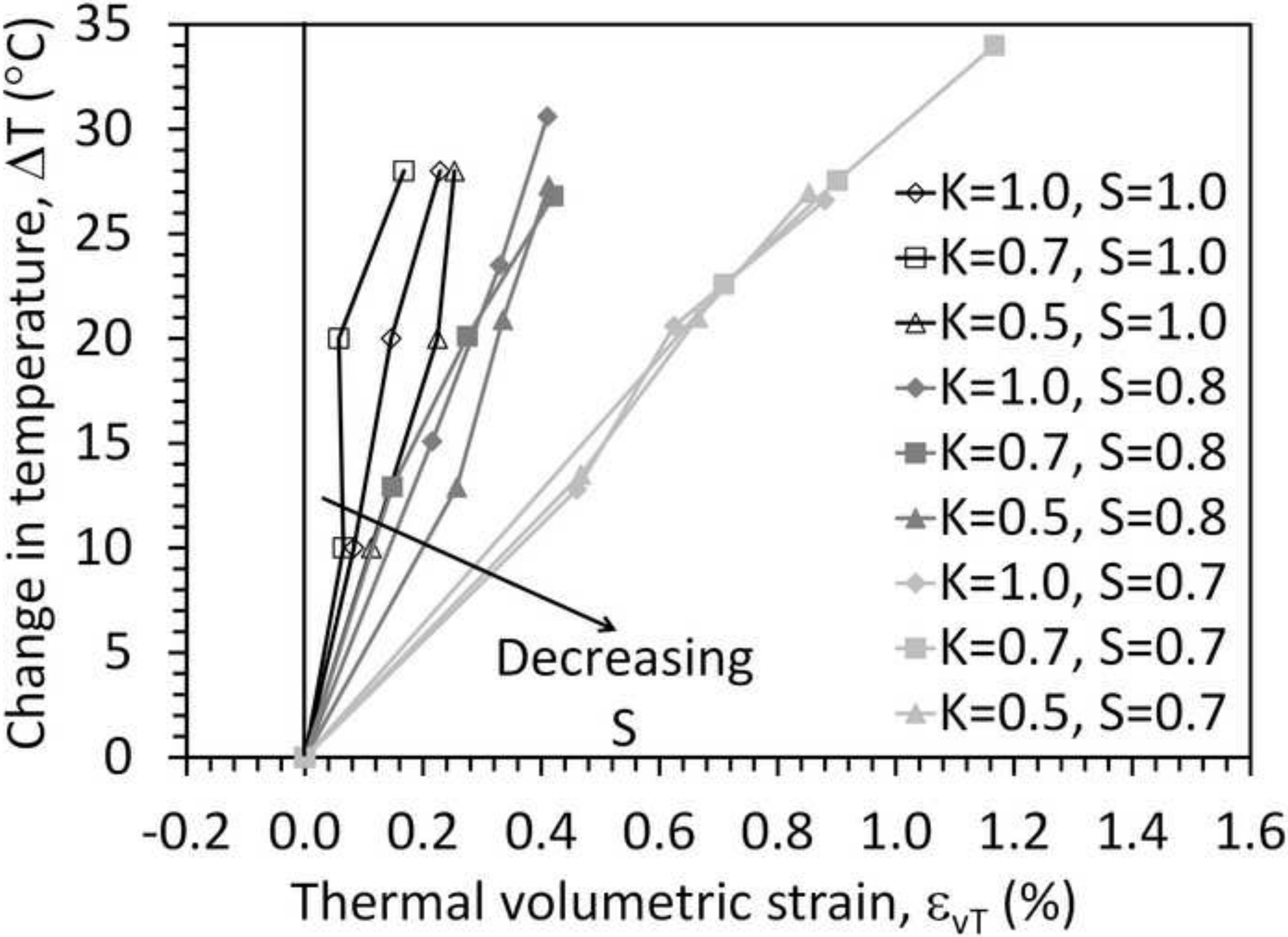

Figure 7
Click here to download high resolution image

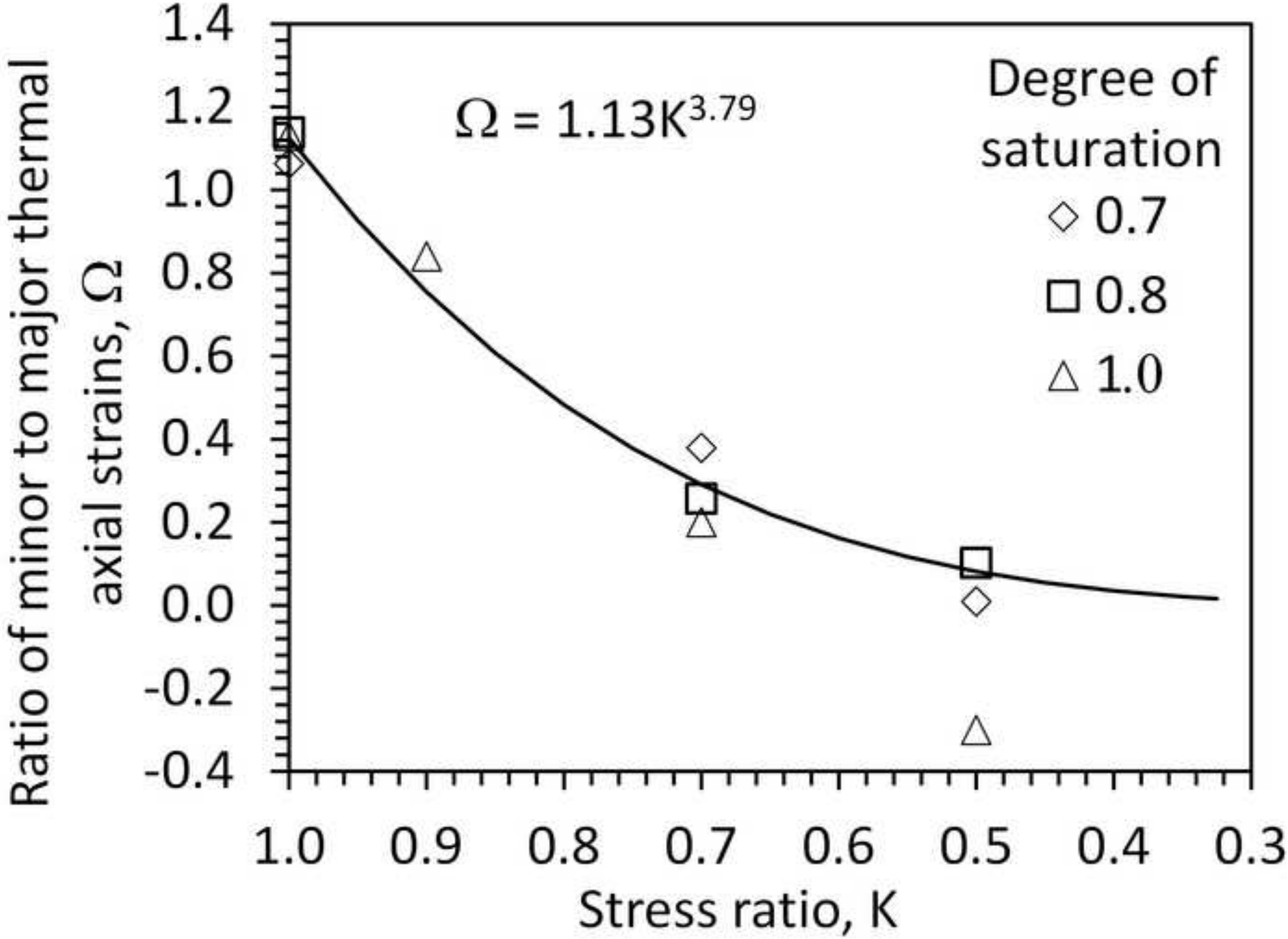

Figure 8

Click here to download high resolution image

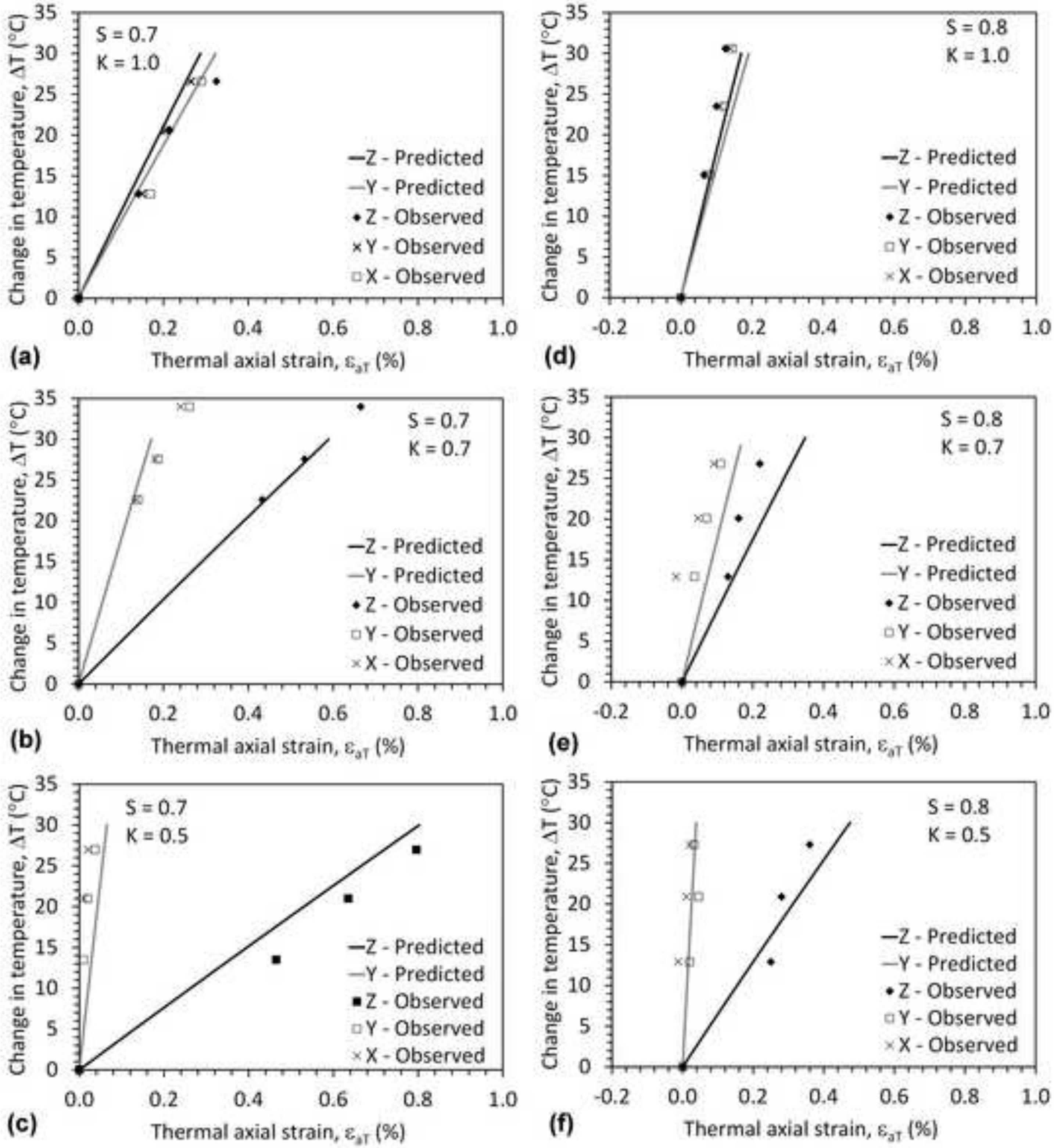

Figure 9
Click here to download high resolution image